6 EXPERIMENTAL PROCEDURE OF THE HGHG FEL

6.1 Introduction

The harmonic generation without exponential amplification in an FEL using a seed laser has previously been analyzed and observed experimentally [35-37]. However, harmonic generation followed by exponential amplification to reach saturation, was first proposed in ref. [38-40] and realized for the first time in this research and reported in [2].

In the High Gain Harmonic Generation experiment the CO_2 laser, modulator and dispersive sections are utilized as described in the ATF overview section. In the SASE case, the radiation starts from the noise. However in the HGHG we start from an initial electromagnetic field.

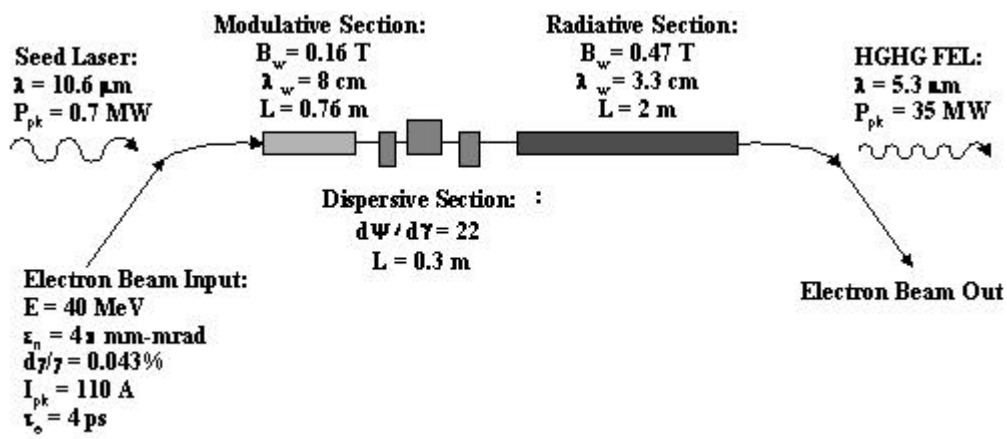

Figure 6-1 Design parameters of the HGHG FEL

The design parameters of the experiment are shown in Figure 6-1[1-2]. The modulator section is a 0.76 m long undulator with a period of 8 cm. The modulator section is tuned to 10.6 μm at electron beam energy of 41.3 MeV. We seed the electrons with 0.7 MW power 10.6 μm CO_2 laser pulse. As mentioned in section 2.2, the energy of the electrons is modulated due to the interaction with the CO_2 laser beam. The length of the modulator is just enough to produce an energy modulation equal to the energy spread of the electron beam but not long enough to produce gain. The energy spread vs. phase is

plotted in Figure 6-2. The vertical width of the plot is the intrinsic energy spread of the electron beam and the sinusoidal curve is the energy modulation.

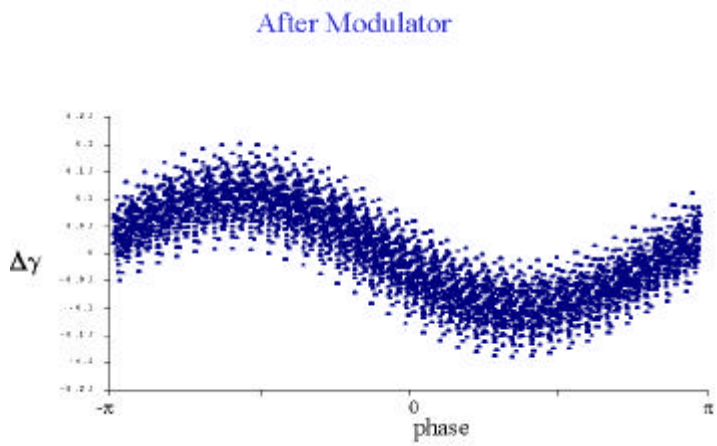

Figure 6-2 Energy modulation vs. phase of the electron beam after the modulator

This energy modulation is converted into density modulation in the dispersive section (three dipole chicane) by the principle that the more energetic electrons will catch up with the less energetic electrons. The plot in Figure 6-3 shows the accumulation of the electrons, the so-called bunching. These micro-bunched electrons are sent to the radiator section, which is tuned for a higher harmonic of 10.6 μm CO_2 laser (in this case 5.3 μm).

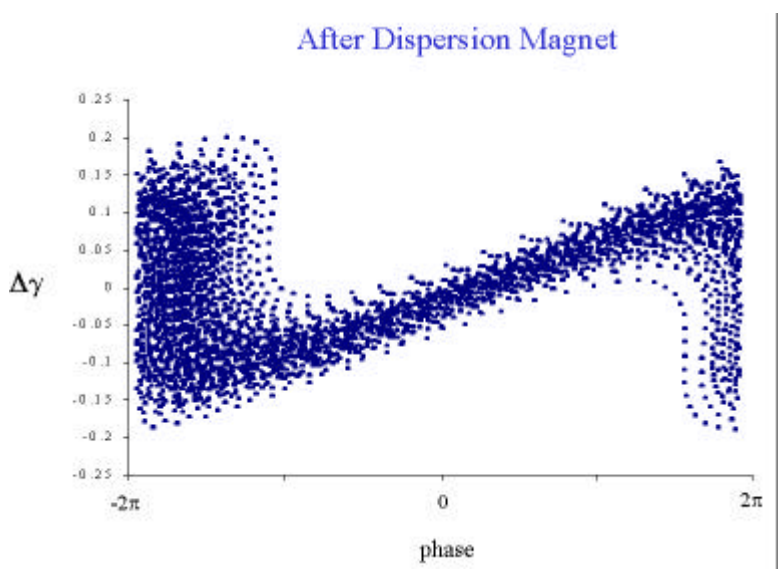

Figure 6-3 Energy modulation vs. phase of the electron beam after the dispersion magnet

In the first part of the radiator the micro-bunched electrons start radiating coherently and in the later parts the radiation is build up and amplified exponentially.

The energy distribution of the electron beam is shown in Figure 6-4 [1]. The projection of the plot below on energy axis shows a double band that means some electrons gain energy but more electrons lose energy. On average, the electrons lose energy, and energy conservation tells us that the FEL radiation gains energy.

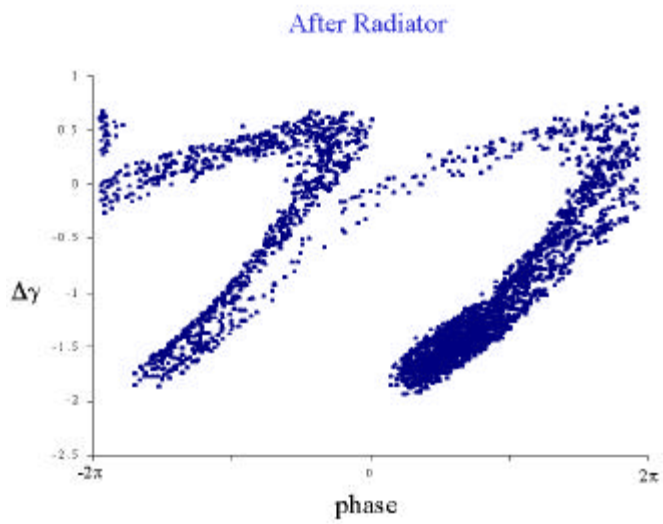

Figure 6-4 Energy modulation vs. phase of the electron beam after the radiator wiggler

The design output of the HGHG radiation is 35 MW.

Spatial and temporal alignment of the electron beam and the CO_2 laser beam is critical for a good interaction in the modulator section.

6.2 Spatial and Temporal Alignment Procedure

6.2.1 Synchronization of the CO_2 Laser with the Electron Beam

Electron beam pulse length is usually 6-8 ps and CO_2 laser pulse length is 100-200 ps. If the two beams were not synchronized there would be no interaction. To synchronize the CO_2 laser pulse to the electron beam we measure electron signal at a stripline beam monitor, located near the modulator section. We also measure the arrival time of the CO_2 laser with an infrared detector. We set up the infrared detector close to

the stripline detector, near the I-POP 1 monitor location. We connect both signals to a fast scope with equal length cables. We adjust the timing of the laser with respect to electron beam by changing the optical delay trombone. This adjustment has to be repeated only if disturbed by another experiment.

6.2.2 Alignment Procedure of the CO_2 Laser

As with so many other elements of the experiment, we use the He-Ne laser to establish the alignment of the CO_2 laser. In the following we will go through the equipment and procedures for guiding the CO_2 laser beam. As mentioned in Chapter 3, three diagnostic stations are located in the area of the modulator section. One diagnostic is located upstream of the modulator, one is in its middle and the other one is downstream of the modulator. Each diagnostic station (or pop in) consists of two CCD cameras, a liquid crystal (LC) and a kinematic remote controlled mirror (see Figure 6-6). The liquid crystal is heat sensitive, and changes color as a function of temperature. As can be seen in Figure 6-6, the kinematic mirror may send the beam either into the I-POP monitor for electron beam diagnostic or to the LC camera for CO_2 alignment. The He-Ne laser beam is used as the reference for alignment of the CO_2 laser beam.

To get the two beams into co-alignment we use the following procedure (see Figure 6-5): We remove the kinematic mirror and measure the positions of the He-Ne at each LC camera. For this purpose the diagnostic stations' kinematic mirrors are set to select the LC cameras. Then the upstream kinematic mirror of Figure 6-5 is inserted, sending the CO_2 laser to the beam line. We measure the positions of the CO_2 laser at each LC camera. We steer the CO_2 laser using the motorized mirror and the kinematic mirror shown in Figure 6-5 to overlap with the He-Ne laser.

Having co-aligned the CO_2 and He-Ne laser beams, we align the electron beam to the He-Ne laser. We retract the kinematic mirror of Figure 6-5 and the diagnostic station kinematic mirrors, allowing the He Ne beam into the I-POP cameras, which also observe the electron beam position. Using the beam line trim magnets located upstream of the modulator, the electron beam is aligned to the He-Ne laser. As a result, we established a good alignment between the CO_2 laser and the electron beam in the modulator section.

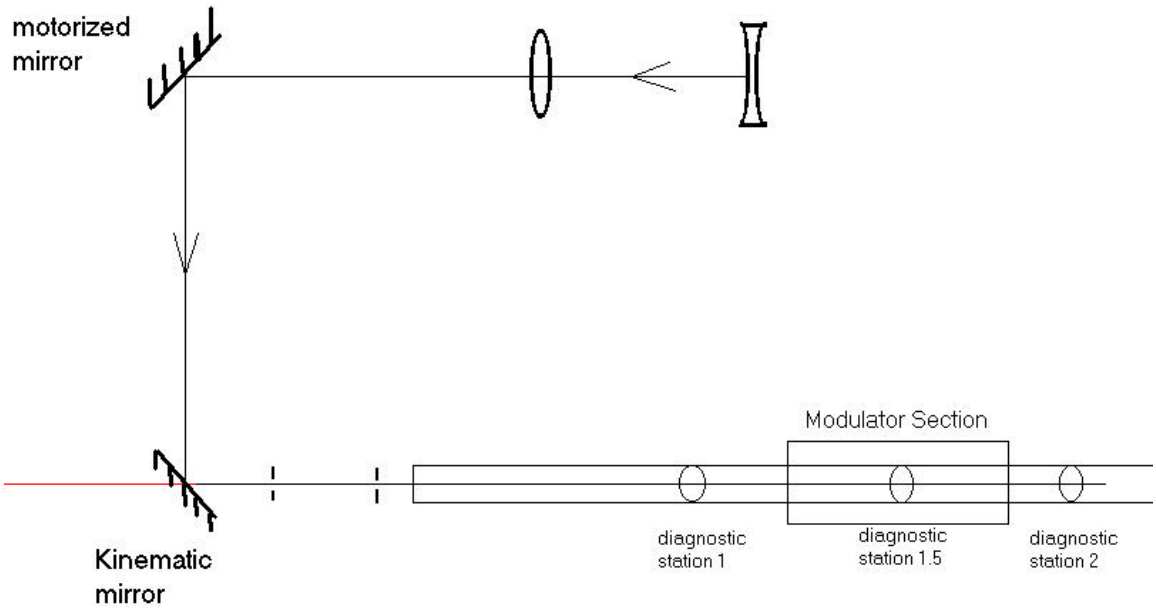

Figure 6-5 CO_2 and He-Ne optical transport line for the modulator section

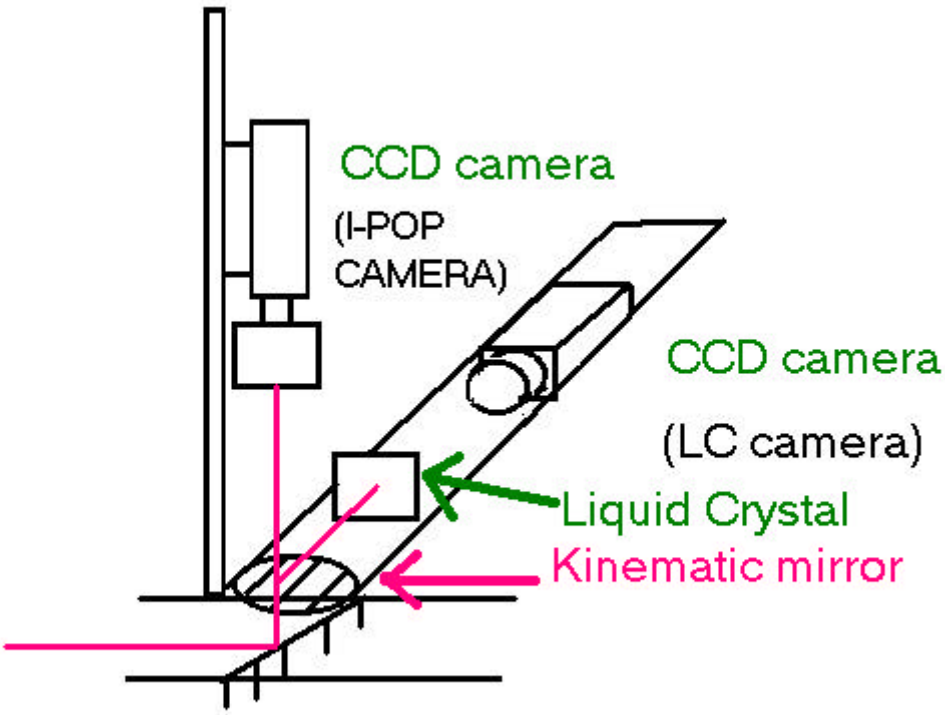

Figure 6-6 diagnostic station for the modulator

6.2.3 Alignment of the Electron Beam in the Radiator

We repeat the same alignment procedure in the radiator section, using He-Ne laser, as described for the SASE case in Chapter 5.

6.3 Measuring the Modulation

Following all these alignment procedures, we start the experiment by measuring the energy modulation of the electron beam by the CO_2 laser. The energy of the laser pulse is about 200 mJ and the power is about 1 GW. Since the laser energy is much more than the design energy for the HGHG process, this will cause the over-bunching in the electron beam. That means the density modulation shown in Figure 6-3 will roll over and deteriorate. Thus the HGHG procedure conditions are not satisfied but there will be a large energy modulation in the electron beam. The dipole after the radiator and a beam monitor equipped with a camera at the end of the beam-line serve as an energy spectrometer. The dipole converts the energy distribution into a horizontal position distribution. In Figure 6-7 the electron beam at the spectrometer camera is shown without the CO_2 laser interaction.

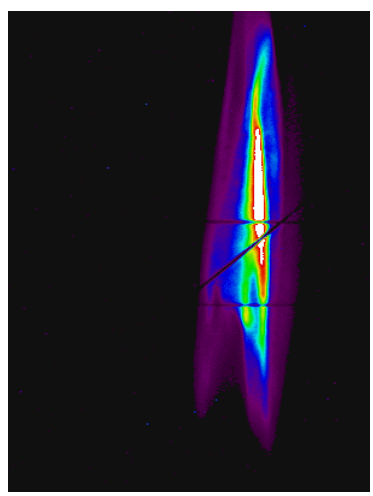

Figure 6-7 Electron beam at the spectrometer with no CO_2 laser interaction. The horizontal axis corresponds to energy; the vertical axis is vertical position.

The electron beam at the spectrometer camera with the various CO_2 laser interactions is shown in Figure 6-8.

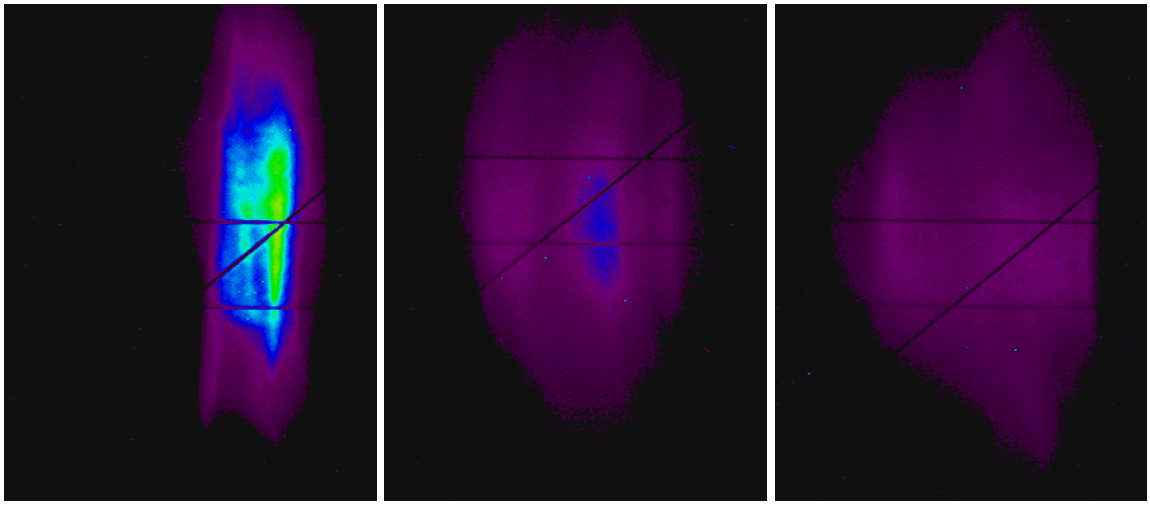

Figure 6-8 Electron beam at the spectrometer with various CO_2 laser interactions. The horizontal axis corresponds to energy; the vertical axis is vertical position.

We use the energy modulation of the electron beam to optimize the temporal and spatial overlap of the laser and electrons. We optimize the optical delay trombone position and alignment of the CO_2 laser by maximizing the energy modulation of the electron beam.

6.4 Measuring the HGHG Output as a Function of CO_2 Power

Following the optimization of the temporal and spatial overlaps; the CO_2 laser power is attenuated gradually towards the design power of 0.7 MW. We reduce the CO_2 laser power by inserting calibrated CaF_2 attenuators into the laser path. For each power setting we measure the HGHG output in the FEL room using a Molectron J3-09 joulemeter [41]. Figure 6-9 shows the results of the measurement and Figure 6-10 shows the simulations [1].

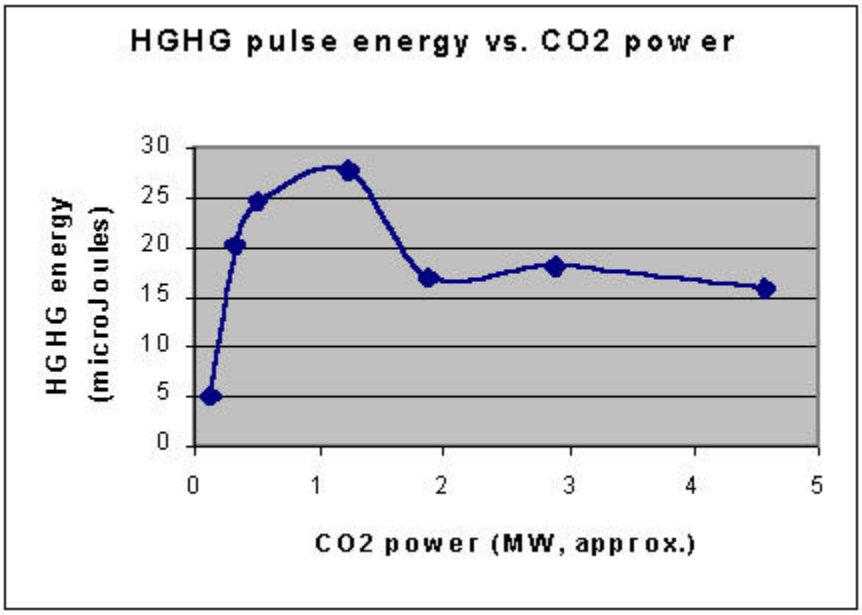

Figure 6-9 Measured HGHG output power vs. CO_2 power plot

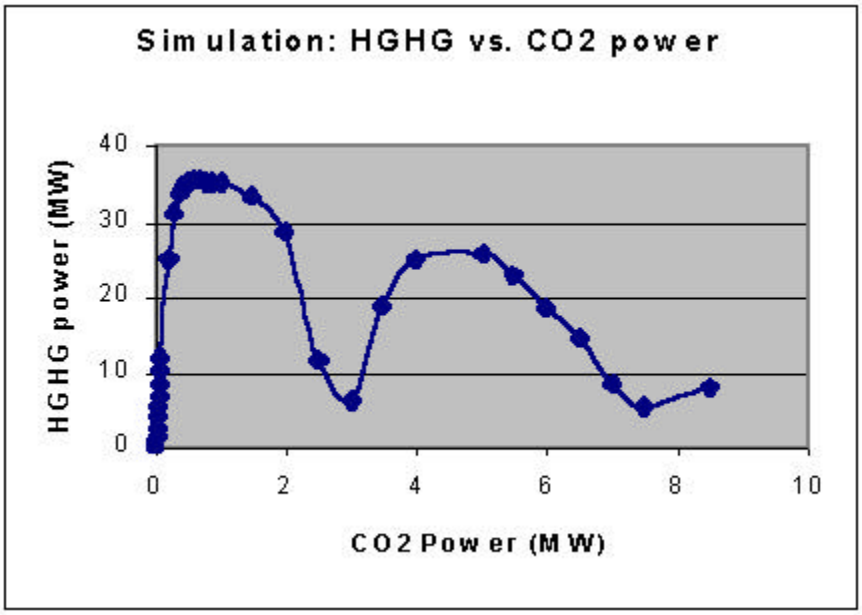

Figure 6-10 Numerical simulation of the HGHG output power vs. CO_2 power

For normal HGHG operation we set the CO_2 power to where we get the maximum HGHG output. Typically we attenuate the CO_2 power by a factor of one thousand to get the maximum HGHG output, which is about 100 μJ. The maximum SASE output that we got was about 10 V signal from the In-Sb detector, which has calibration of 20 pJ/V.

Thus the SASE output is about 200 pJ energy. Therefore the HGHG output is larger than the SASE output by a factor ~10^6. Also the spontaneous radiation is less than the SASE by a factor 10-50. Thus the HGHG output is larger than the spontaneous radiation by a factor of ~10^7.

The simulation [42] of the HGHG power as a function of distance in the radiator wiggler is shown in Figure 6-11. The curve at the end of the wiggler indicates the saturation of the FEL process.

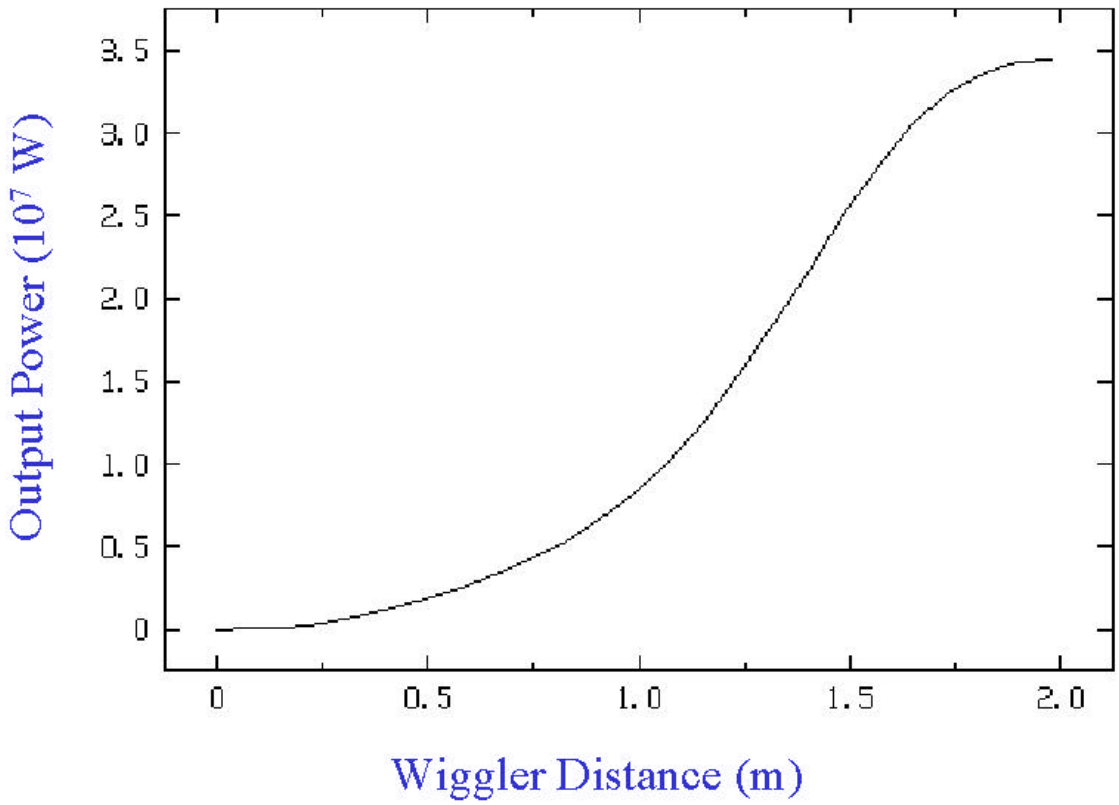

Figure 6-11 Numerical simulation result of the output power vs. wiggler distance

7 SPECTRUM MEASUREMENT OF HGHG FEL

7.1 Multi-Shot Spectrum Measurement of the HGHG Output

The spectrum of HGHG signal can be measured similarly to the SASE spectrum discussed above. We set the spectrometer output slit to an opening of 0.2 mm, corresponding to a maximum dispersion of 5 nm. Since the repetition rate of the CO_2 laser is every 15 sec. the measurement takes a longer time than the SASE measurement. We did not use any automated program because of this low repetition rate. We manually changed the wavelength of the spectrometer and record the signal. We split the HGHG output as shown in Figure 7-1. Part of the beam goes to the joule-meter to normalize the signal and the other part goes to the spectrometer.

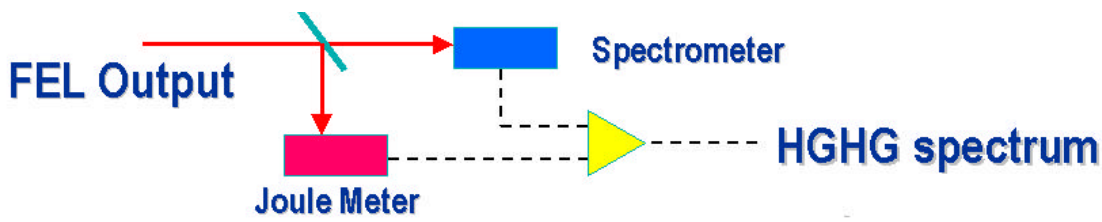

Figure 7-1 Spectrum measurement schematic layout

In this case we did not use averaging thus every point is a single shot. We used about 10^6 times attenuation to measure the signal with the In-Sb detector. The result of the spectrum measurement is shown in Figure 7-2[1,2,42]. The width of the spectrum is about 20 nm, which is much narrower than the SASE spectrum width (150 nm).

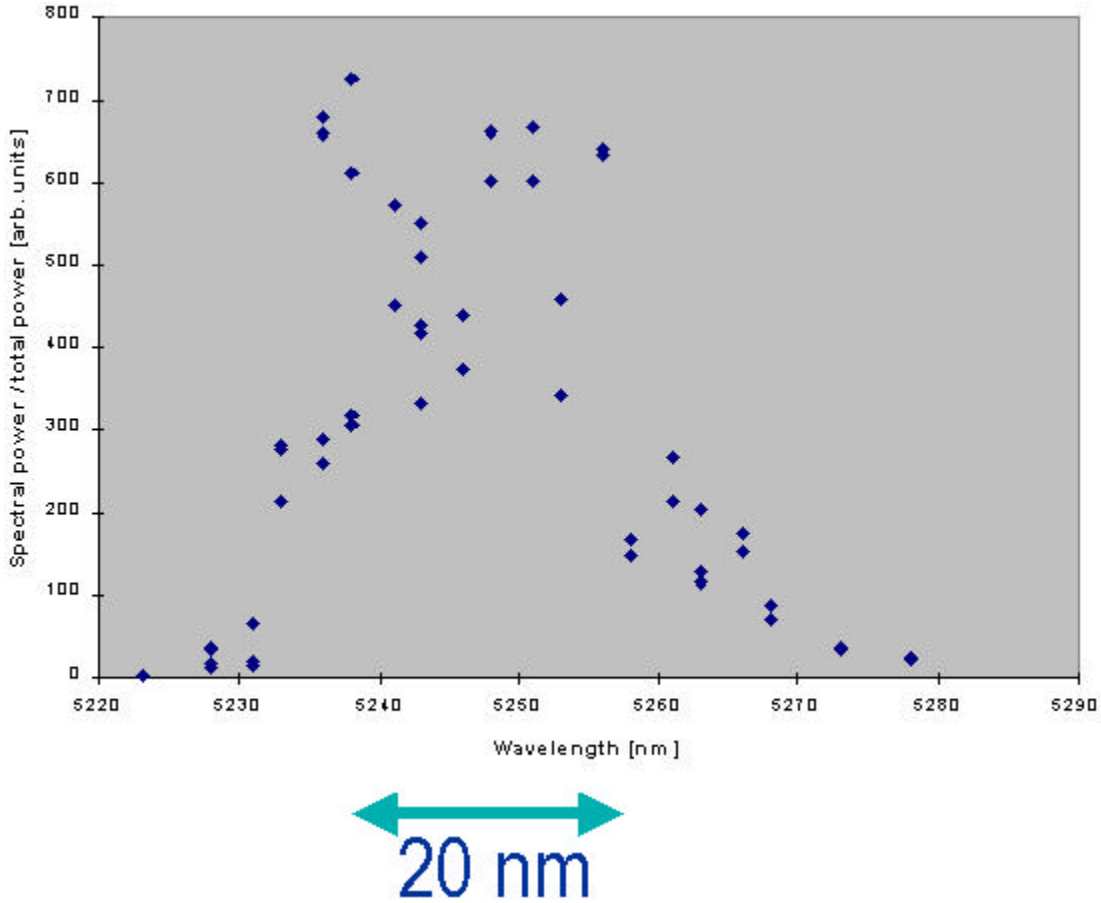

Figure 7-2 Multi-shot spectrum measurement of the HGHG signal

7.2 Single Shot Spectrum Measurement of the HGHG Output

The large scatter of the multi-shot spectrum measurement is due to shot-to-shot fluctuations of various parameters of the experiment, such as the CO_2 laser power, the electron beam current, pointing jitter, etc. We use the high power of the HGHG signal to our advantage in taking a single shot measurement. With this high power, we could use the Pyroviewer infrared camera, placed at the spectrograph port of the spectrometer.

The resolution of the camera was measured using an imaging technique (see Figure 7-3). An image of a test pattern (resolution target) is formed the on the pyroviewer camera using a He-Ne laser. The test pattern has groups of parallel lines with various spacing between them.

We used a 10 cm focal length lens to form the image of the target.

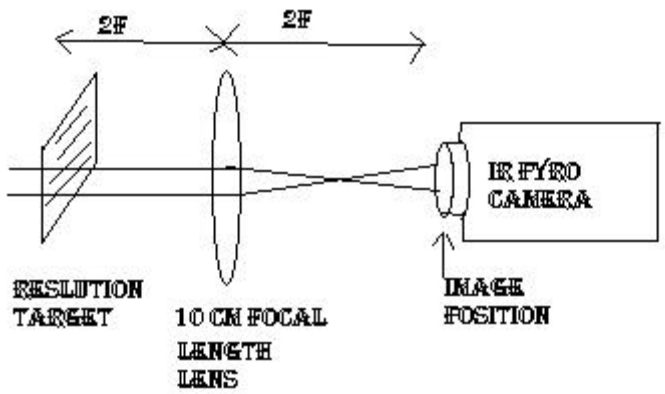

Figure 7-3 Resolution Measurement Schematic Layout

We were able to resolve 0.16 mm vertically and 0.19 mm horizontally. Thus the camera has a better resolution in its vertical direction. Since the spectrometer disperses horizontally, what we really need is horizontal resolution, and the camera was mounted such that its vertical axis was in the horizontal plane of the spectrometer.

We retracted the second kinematic mirror in the spectrometer to direct the radiation to the camera. Next, we used a He-Ne laser to calibrate the spectrometer. The question is how much movement on the camera corresponds to a given wavelength shift. In the camera's vertical axis the calibration of the camera is 53 μm/pixel. We set the spectrometer to certain wavelength and measure the position of the beam. Then we shift the wavelength setting and measure the position of the beam again. This calibration turns out to be 1.33 pixel/nm. Combining this result with the camera calibration we get 70 μm/nm, which means that a 1nm wavelength shift corresponds to a 70 μm shift on the camera. Since the measured resolution of the camera was 160 μm, this corresponds to a wavelength resolution of 2.3 nm. It turns out that this resolution is better than what we obtained in the multi-shot measurement!

Following these calibrations we measured the spectrum of the HGHG output. The expanded view of the beam profile on the pyroviewer camera is shown in Figure 7-4.

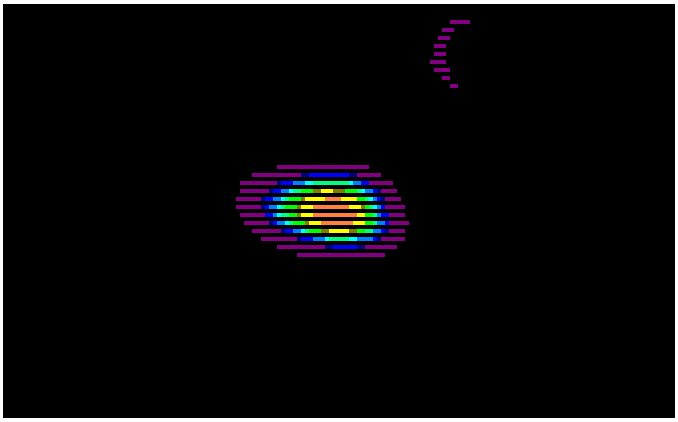

Figure 7-4 Single-shot spectrum image of the HGHG output. The vertical axis corresponds to wavelength; the horizontal axis shows the vertical beam size.

The vertical axis in Figure 7-4 corresponds to the spectrum distribution of the HGHG output. We analyzed the central slice of the beam and converted pixels to nm and plotted in Figure 7-5 [2].

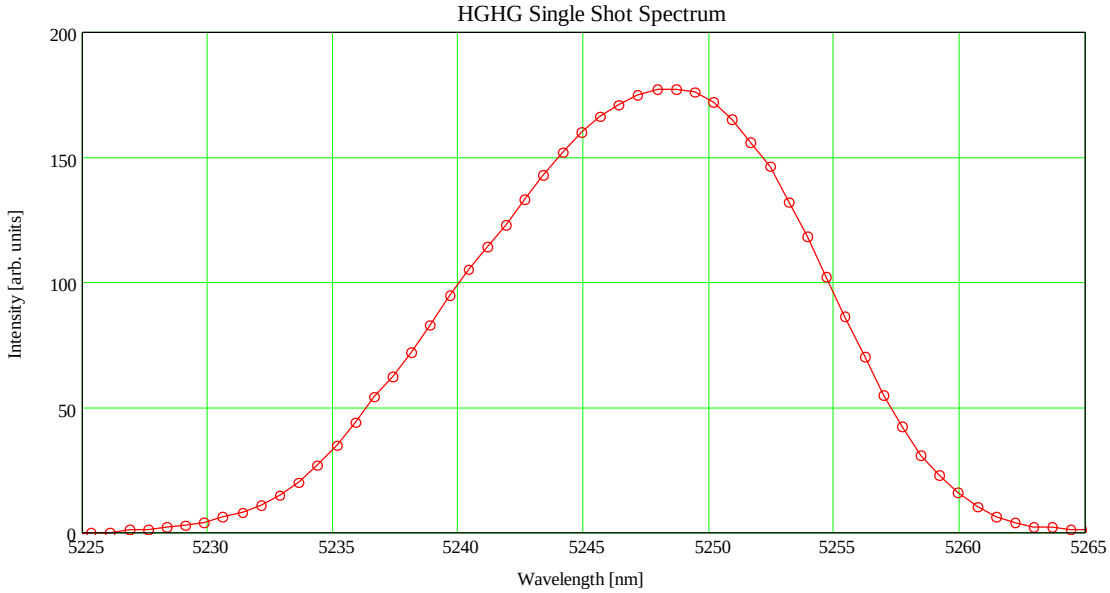

Figure 7-5 Single-shot spectrum of the HGHG output

The FWHM of the spectrum curve is about 15 nm, which is consistent with the multi-shot HGHG spectrum measurement. The comparison between the SASE, multi-

shot and single-shot spectrum measurements are shown in Figure 7-6. The upper plot is multi-shot SASE (amplified by 10^6) and HGHG spectrum; the lower plot is a single-shot HGHG spectrum.

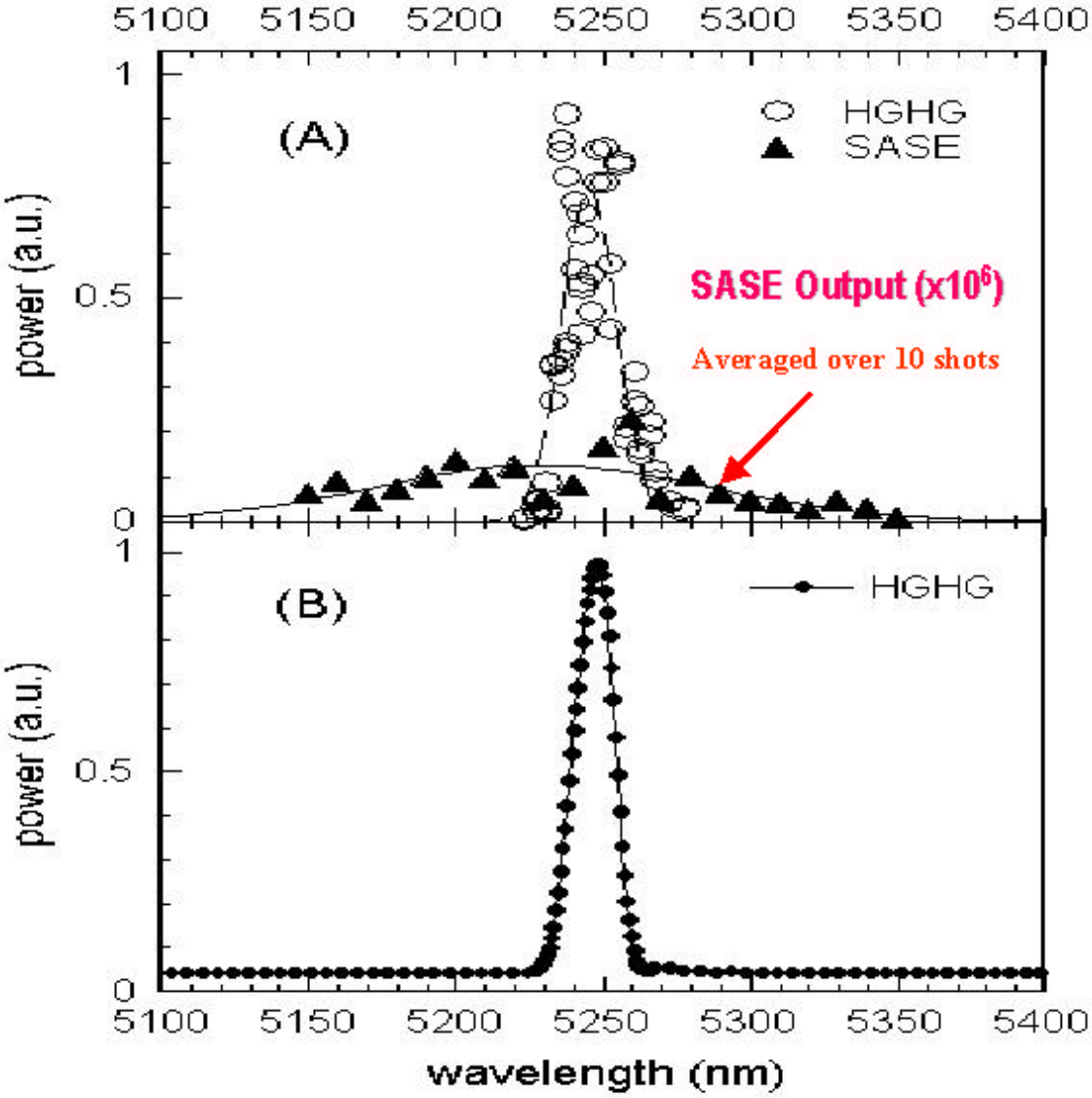

Figure 7-6 Comparison of SASE, Multi-shot HGHG and single-shot HGHG spectrum plots